

In-situ

K C , W X , L ,*, L H , C , L , L ,
W , K E , L L , X G , T P J

Gemological Institute, China University of Geosciences, Wuhan 430074, PR China
 Hubei Gem and Jewelry Engineering Technology Research Center, Wuhan 430074, PR China
 School of Materials Science and Engineering, Huazhong University of Science and Technology, Wuhan 430074, PR China
 Mechanical Engineering, University of Birmingham, Birmingham B15 2TT, UK
 School of Electrical and Electronic Engineering, Huazhong University of Science and Technology, Wuhan 430074, PR China
 WMG, Materials Engineering Centre, University of Warwick, CV4 7AL Coventry, UK

ARTICLE INFO

Keywords:

T
C
S
C
B

ABSTRACT

C , - (3DG) . H
(SLM) (3D)
G in-situ (CVD) C
SLM 3DG ff A CVD
ff T 3DG/ ff ()
(EMI) 88% 27% SE 32.3 B EMI ffi-
(SE) 47.8 B 2.7 GH 2-18 GH .
T SLM .

1. Introduction

G , sp^2
(2630 2^{-1}) 1 ,
(2 10^5 2^{-1} V $^{-1}$ -1)
(65000 W $^{-1}$ K $^{-1}$) 2 . H , π - π
(2D)
3 . A
C
(3DG)
fi (60.6 $^{-2}$) 4
(699.7%), fi
(2DG), 4 , 5 , 6,7 ,
Y (EMI) 8
3DG 9 , 10 ,
11 , 12
H . F
ff 13 . S
()
14 . D
15 . M
CVD
16 . B

*C : G I , C U G , W 430074, PR C .
E-mail address: @ . (.L).

↓ . T
 (. , ↓) , fl (. , , fi ↓ -
 3DG ↓ ,) 3DG. B ↓ , ↓ -
 (. , ↓ , , ↓) . H ↓ , ffi ↓
 ↓ ↓ ↓ ↓ ↓ ↓ ↓ ↓ ↓ ↓ N ↓
 ↓ ↓ ↓ ↓ ↓ ↓ ↓ ↓ ↓ ↓ ↓ ↓
 H ↓ ↓ ↓ ↓ ↓ ↓ ↓ ↓ ↓ ↓ ↓ ↓
 S ↓ ↓ ↓ ↓ ↓ ↓ ↓ ↓ ↓ ↓ ↓ ↓
 (AM) / (SLM), ↓ ↓ ↓ ↓ ↓ ↓ ↓ ↓ ↓ ↓
 ↓ ↓ ↓ ↓ ↓ ↓ ↓ ↓ ↓ ↓ ↓ ↓ ↓ ↓
 fl ↓ ↓ ↓ ↓ ↓ ↓ ↓ ↓ ↓ ↓ ↓ ↓ ↓ ↓
 in-situ SLM ↓ ↓ ↓ ↓ ↓ ↓ ↓ ↓ ↓ ↓ ↓ ↓
 ↓ ↓ ↓ ↓ ↓ ↓ ↓ ↓ ↓ ↓ ↓ ↓ ↓ ↓ ↓ ↓
 21 , N ↓ ↓ ↓ ↓ ↓ ↓ ↓ ↓ ↓ ↓ ↓ ↓ ↓ ↓
 22 . C T ↓ ↓ ↓ ↓ ↓ ↓ ↓ ↓ ↓ ↓ ↓ ↓ ↓ ↓
 ↓ ↓ ↓ ↓ ↓ ↓ ↓ ↓ ↓ ↓ ↓ ↓ ↓ ↓ ↓ ↓
 . C N ↓ ↓ ↓ ↓ ↓ ↓ ↓ ↓ ↓ ↓ ↓ ↓ ↓ ↓
 CVD ↓ ↓ ↓ ↓ ↓ ↓ ↓ ↓ ↓ ↓ ↓ ↓ ↓ ↓ ↓ ↓
 ↓ ↓ ↓ ↓ ↓ ↓ ↓ ↓ ↓ ↓ ↓ ↓ ↓ ↓ ↓ ↓
 (< 0.001 . %) ↓ ↓ ↓ ↓ ↓ ↓ ↓ ↓ ↓ ↓ ↓ ↓ ↓ ↓
 (> 0.1 . %) 17 , 23 . W ↓ ↓ ↓ ↓ ↓ ↓ ↓ ↓ ↓ ↓ ↓ ↓ ↓ ↓
 SLM ↓ ↓ ↓ ↓ ↓ ↓ ↓ ↓ ↓ ↓ ↓ ↓ ↓ ↓ ↓ ↓
 24 . H ffi ↓ ↓ ↓ ↓ ↓ ↓ ↓ ↓ ↓ ↓ ↓ ↓ ↓ ↓
 (1000-1100) . F fl ↓ ↓ ↓ ↓ ↓ ↓ ↓ ↓ ↓ ↓ ↓ ↓ ↓ ↓
 SLM ↓ ↓ ↓ ↓ ↓ ↓ ↓ ↓ ↓ ↓ ↓ ↓ ↓ ↓ ↓ ↓
 T ↓ ↓ ↓ ↓ ↓ ↓ ↓ ↓ ↓ ↓ ↓ ↓ ↓ ↓ ↓ ↓
 SLM ↓ ↓ ↓ ↓ ↓ ↓ ↓ ↓ ↓ ↓ ↓ ↓ ↓ ↓ ↓ ↓
 . A ↓ ↓ ↓ ↓ ↓ ↓ ↓ ↓ ↓ ↓ ↓ ↓ ↓ ↓ ↓ ↓
 SLM ↓ ↓ ↓ ↓ ↓ ↓ ↓ ↓ ↓ ↓ ↓ ↓ ↓ ↓ ↓ ↓

8 9.8(.3(↓ 445.3, . ↓ .2)-3)-412.1()-414.6()-840.8 J/TIT

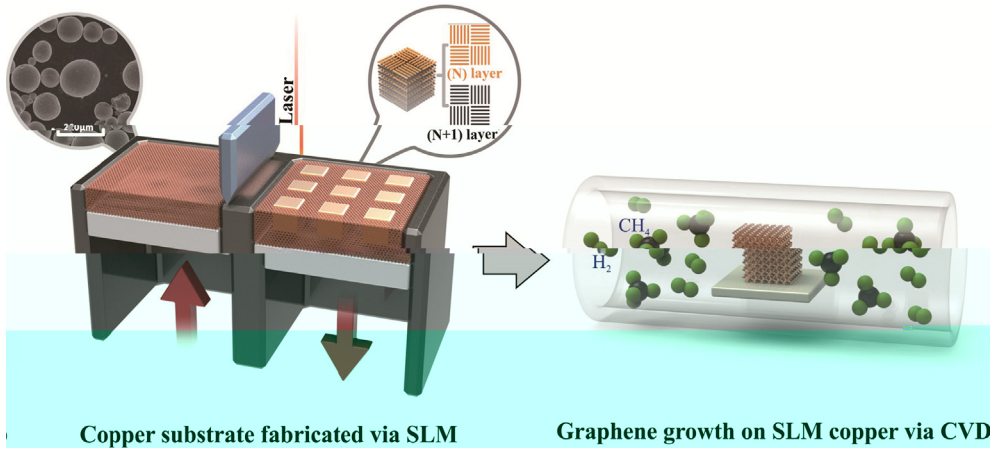


Fig. 1. Schematic of the manufacturing process. The left part shows the SLM process for fabricating a copper substrate with a grid pattern. The right part shows the in-situ CVD process for growing graphene on the SLM copper substrate. The CVD process involves the reaction of CH₄ and H₂ gases at high temperature to deposit graphene layers on the copper substrate.

3. Results and discussion

3.1. Formation of SLM copper

3.1.1. SLM manufacturing of copper under different line energy densities

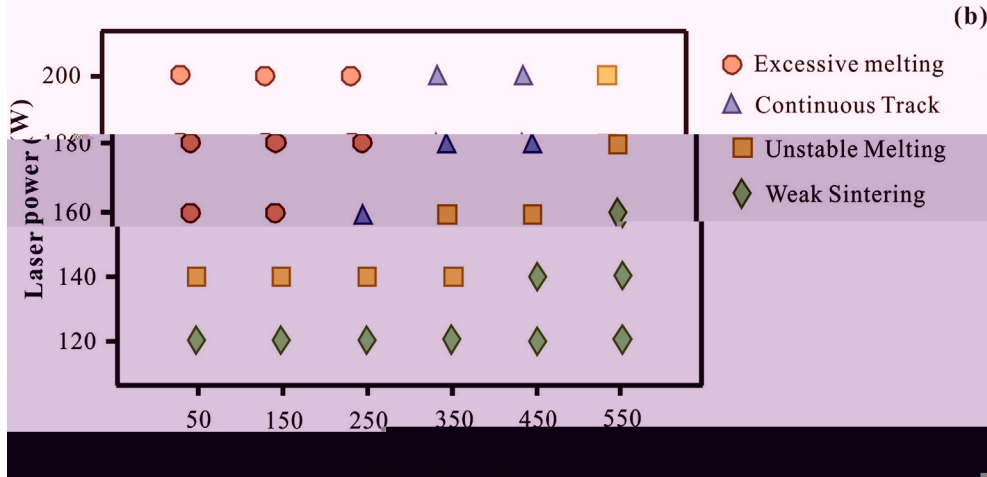
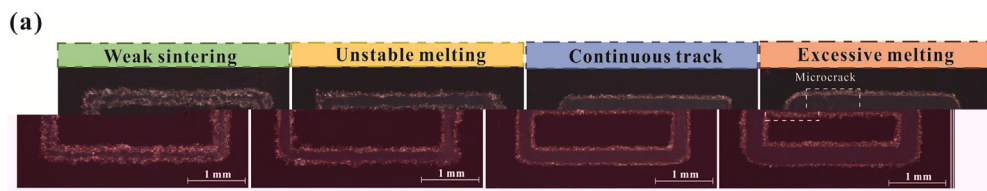


Fig. 2. SEM images of SLM copper tracks under different laser conditions. (a) SEM images of SLM copper tracks under different laser conditions. (b) Scatter plot of Laser power (W) vs. Laser speed (mm/s) for different SLM conditions.

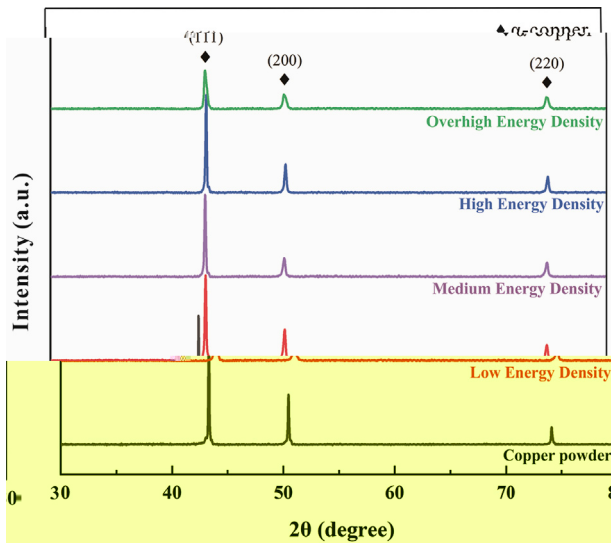


Fig. 3. XRD

3.1.2. Formation of anisotropic microstructure under different volumetric energy density

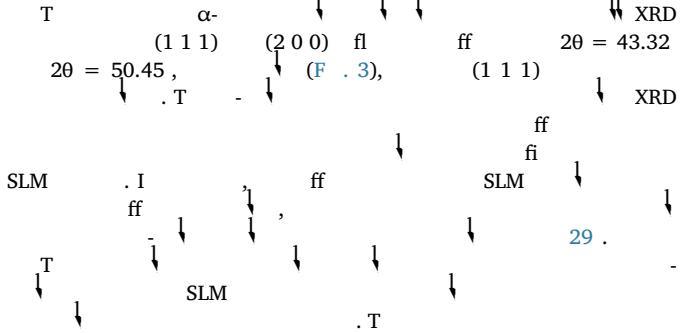


Fig. 4. O

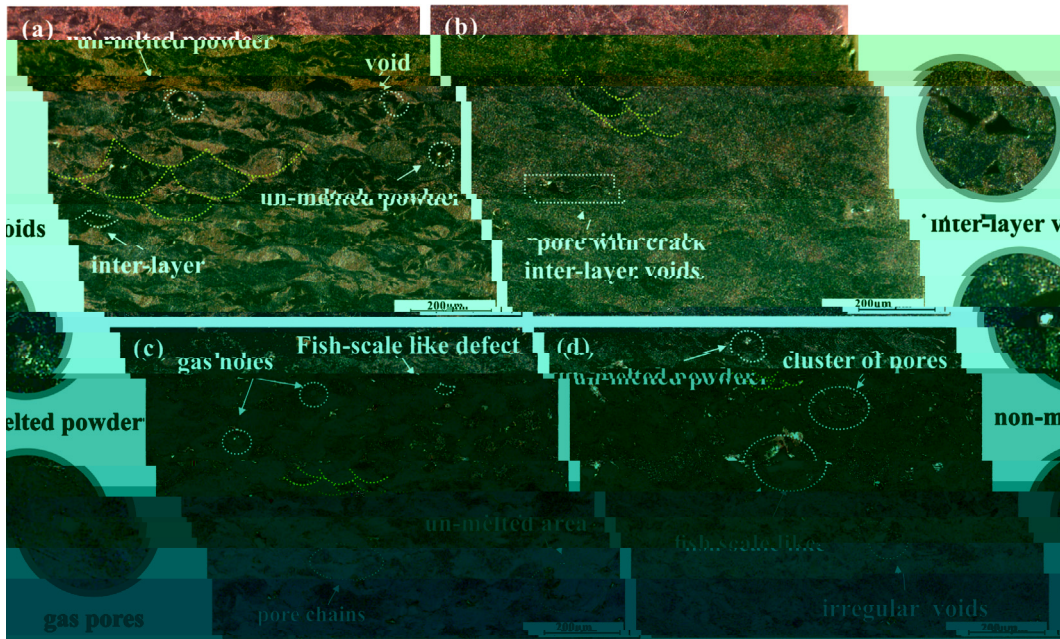


Fig. 4. O (285 J/cm³), (128 J/cm³), (3000 J/cm³), (857 J/cm³)

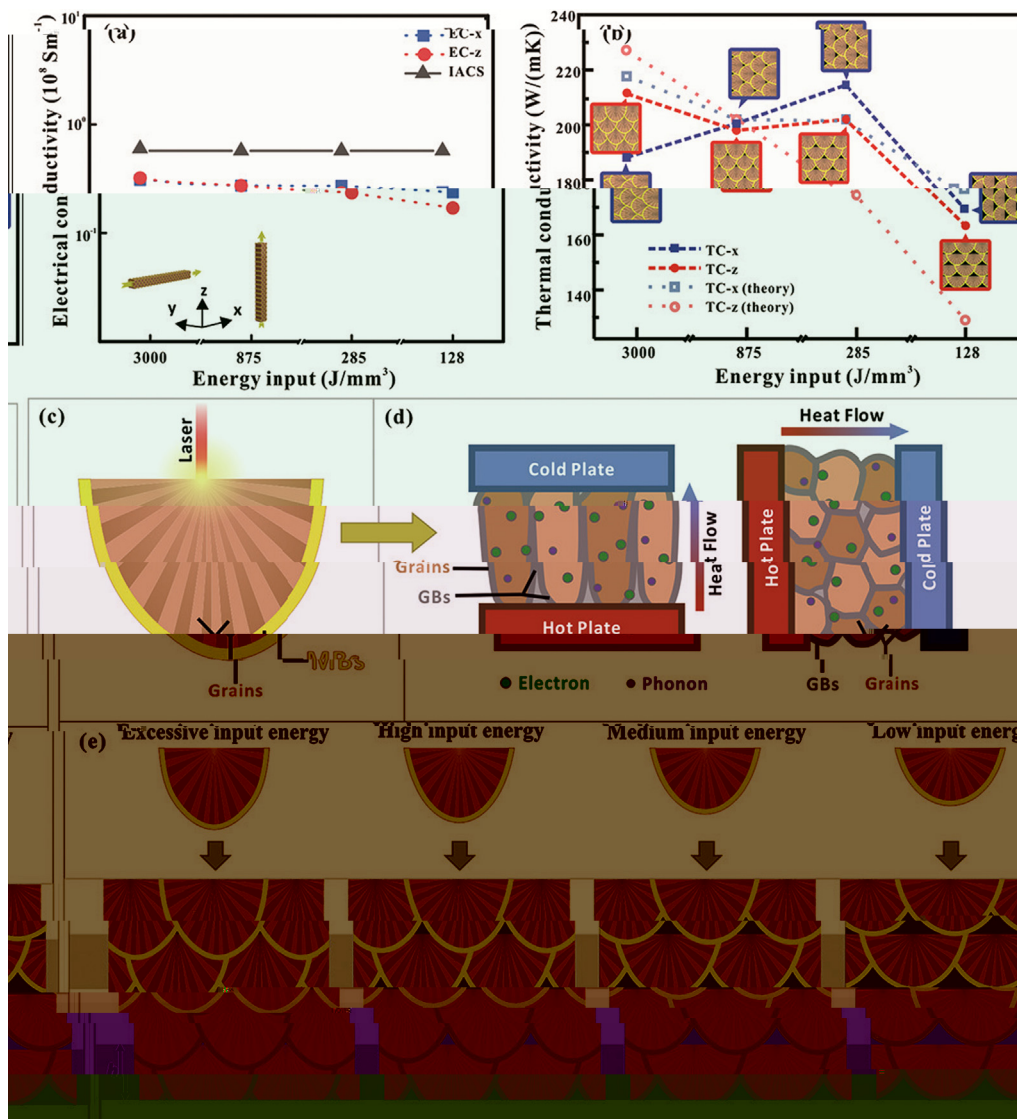


Fig. 7. (a) Electrical conductivity vs energy input for EC-x, EC-z, and IACS. (b) Thermal conductivity vs energy input for TC-x, TC-z, and theoretical values. (c) Schematic of laser irradiation on a material. (d) Schematic of heat flow through a material with grains and grain boundaries (GBs) between hot and cold plates. (e) Schematic showing the effect of excessive, high, medium, and low input energy on the material's structure.

3.3. Morphology and structure of CVD 3DG/Cu porous scaffolds

SEM, 3DG/C, 450 μm (F. 8a), A, SEM, 3DG/C, 450 μm (F. 8b), EDS, (F. 8c-d), SEM, 3DG/C, 450 μm (F. 8e-g), T, 3DG/C, 450 μm (F. 8h). (~ 1590 cm^{-1}), 2D- (62699 cm^{-1}), 42 (F. 8). S, (~ 1350 cm^{-1}) D, G, (I_D/I_G).

in-situ CVD, 39, A, 33, V, (25, V), 39, U, N, L, 40, 23, CVD-, 41, 43, D, G, (I_D/I_G).

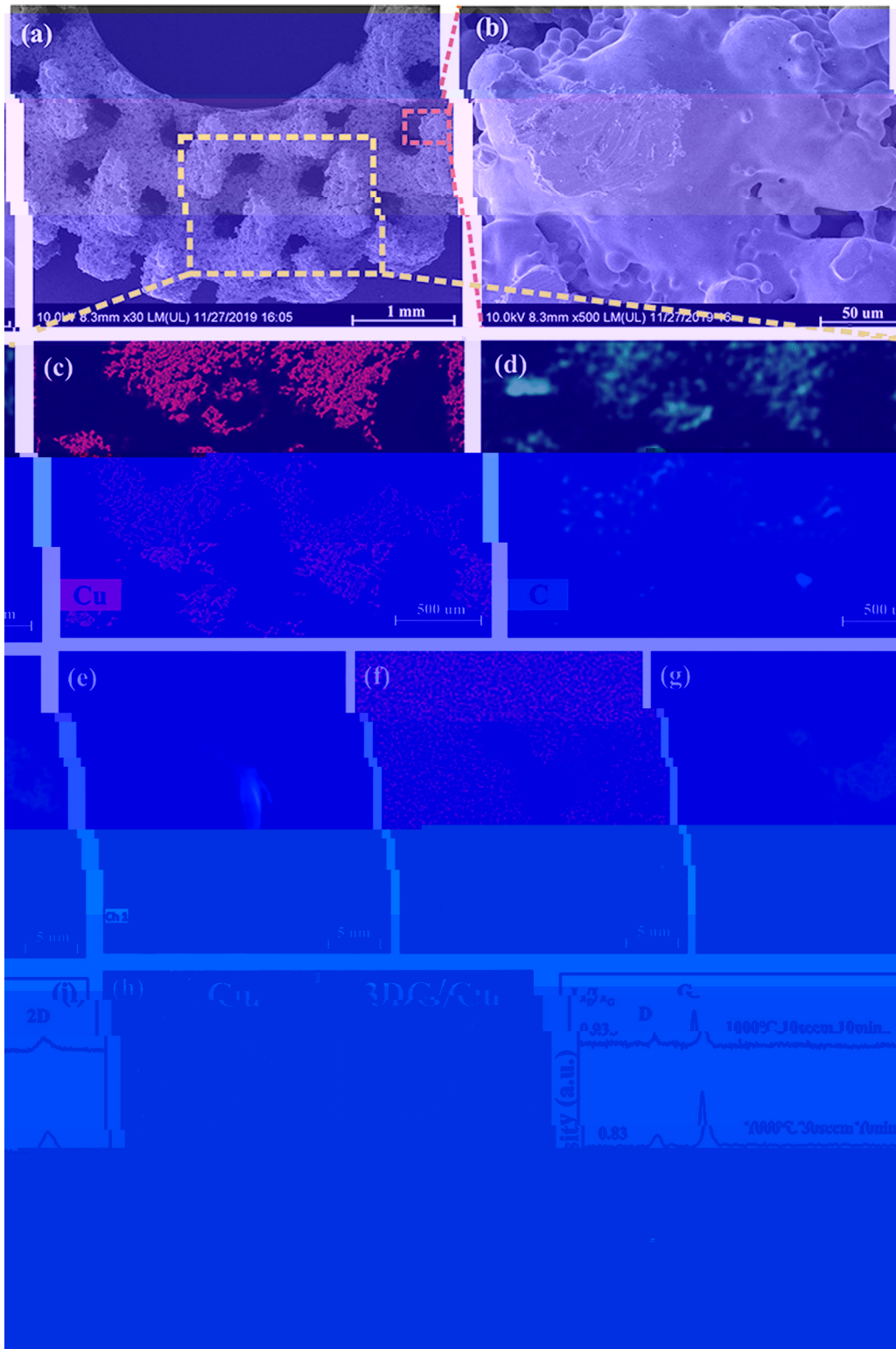


Fig. 8. (a) SEM image of the scaffold at 1 mm scale. (b) High-magnification SEM image of the scaffold at 50 μm scale. (c) EDS map for Cu. (d) EDS map for C. (e) EDS line scan for Cu. (f) EDS line scan for C. (g) EDS line scan for Cu and C. (h) Raman spectrum of 3DG/Cu showing D and G bands.

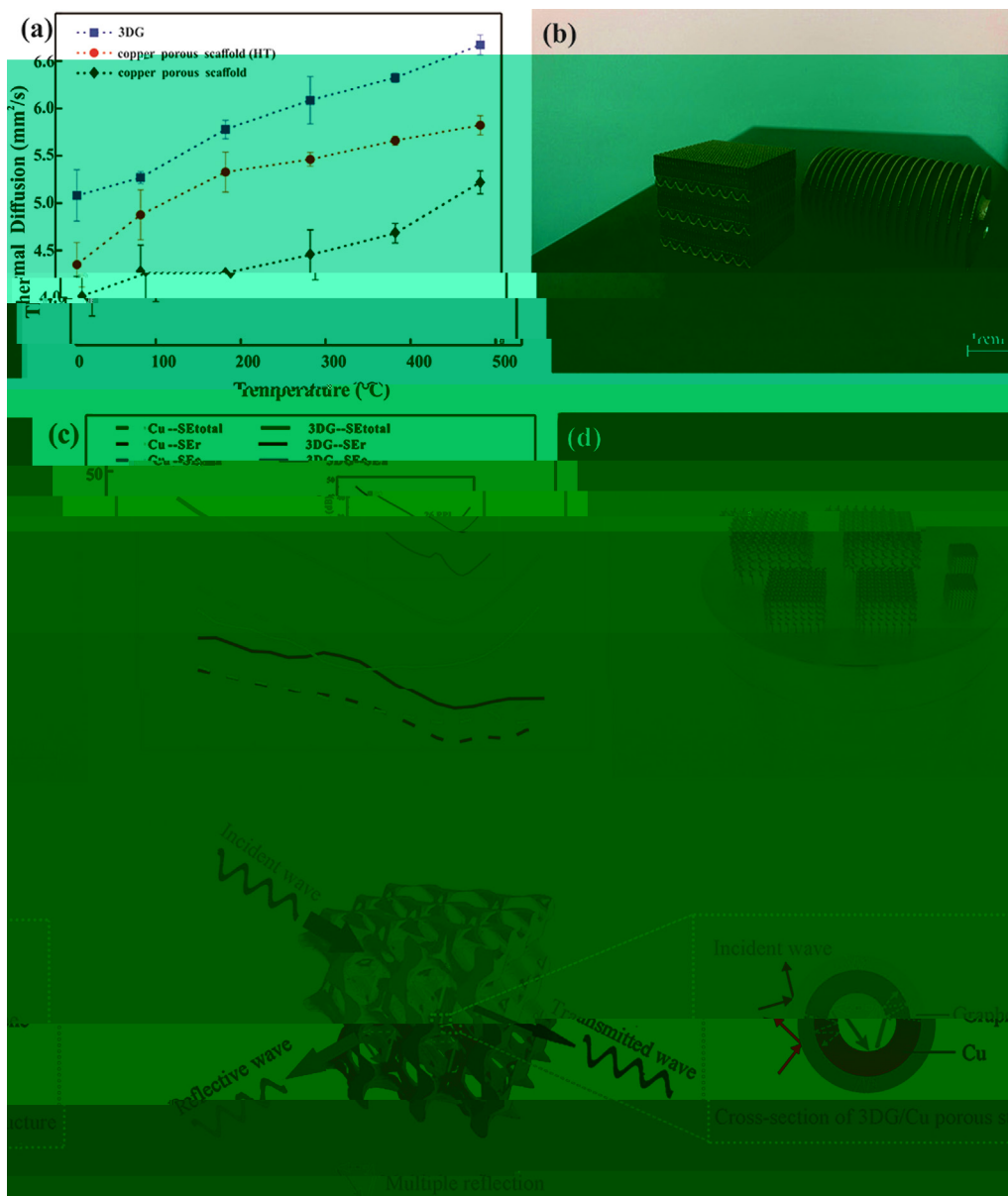


Fig. 9. P 3DG/C ff ; () ff ; () SLM ff ff () S 3DG/C fl EMI. (F

Table 1

Coating materials	Substrate	Method	Maximum shielding efficiency (dB)	Improvement of thermal property (%)	Ref
G	G	I + + ↓ + ↓	37	-	50
G	PS	H - ↓ ↓ ↓	29.3	-	56
G	PMMA	S ↓ + ↓ +	19	-	57
C /G	/C	A ↓ S fi + ↓ ↓ ↓	-	8.5	58
G	N	F + CVD	-	554	59
G	C -N	H ↓ ↓ + ↓	20	-	60
G	C	P + CVD	-	2.4	61
G	C	F - + ↓ ↓	47	6.3	62
G	C	CVD + SLM	47.8	27	T

Note: ↓ (↓ ↓)-PPMA, ↓ -PS.

HT
in-situ (F . 9a). S
 3DG/C ff
 HT
 1-2 . I ,
 . W
 SLM fl
 (F . 9b),
 500 μ)
 . G
 (T 1). I
 N
 T
 EMI, EMI SE,
 (EM)
 2-18 GH (F . 9c),
 . W *in-situ*
 SE
 ff 47.8 B (88.2%)
 3DG/C
 . J K
 44
 EMI
 . T EMI SE
 133%
 R J K 45) 20 110 PPI ()
 EMI
 . W
 17 26 PPI (F . 9c insert) 105%
 EMI SE. I , EMI
 ff
 3DG/C 26 PPI
 32.3 B, 99.9%
 (30
 3DG/C T 1. I
 3D
 T
 (SE_a) fl EMI fl (SE_r),
 (EM) 47 ,
 48 . R 49
 T
 50 . R EMI
 C 51 . F
 52 S O₂ 53 . W

SE_r SE_a
 fi
 F . 9e. W
 3DG/C ff
 fl
 3DG/C
 fi
 EM fi
 EM
 SE_r. O
 EM
 EM
 . T
 44 . T
 3D
 EM
 CVD
 . I
 R S 3.3
 EM
 55 . I
 . O
 3DG/C
 ff
 . T

4. Conclusions

A 3DG/C ff
in-situ CVD
 T ff
 . W 3DG/C
 EMI SE
 15.9 (32.3 B,
 47.8 B (88.2%)), 26.8%
 ff . T 3DG/C
 fl
 . T J
 3DG/C
 EMI ff

Credit authorship contribution statement

Kaka Cheng: C , M , F ,
 W . Wei Xiong: V , I , W ,
 . Yan Li: W & , F ,
 R , S . Liang Hao: F . Chunze Yan:
 R , F . Zhaoqing Li: V . Zhufeng Liu:
 F , . Yushen Wang: I , S . Khamis Essa:
 W - & . Li Lee: D . Xin Gong: S .
 Ton Peijs: W - & , S .

Declaration of Competing Interest

T fl

Acknowledgement

T N N S F N . 51671091, N . 51902295, N . 51675496). T F R F U G (W) (N . (N . CUG170677) H P N S F (N . 2019 CFB264).

Appendix A. Supplementary data

S /10.1016/J .2020.105904. //

References

1 B RG, N N, M K, M S. G : 2018;91:24-69.
2 B AA, G S, B W, C L, T D, M F, S 2008;8(3):902-7.
3 L H, C M, P H, P O, S L G, I 2016;8(36):24112-22.
4 K M, K J, J B, C K, JH, A JH. G . ACS N 2017;11(8):7950-7.
5 P C M, H M, T M, L D. P 2020;262:118266-76.
6 L XJ, W, C LL, J SH, W G, L C-G 2017;101:50-8.
7 HQ, L SW, C LH, J SH, H HQ. S . JM C A 2018;6(42):21216-24.
8 D TM, S P, D P, K J, K M, A T, 3D 2017;1(4):467-70.
9 Q L, L L, T H. P C. P 2014;4(72):38273-80.
10 D X, H L SP, N, W JG. 3D M S2 : P 2016;90:424-32.
11 L XL, XW, S CO, H MK, X HL, D W, S 3D fi EM 2018. // /10.1002/ 201803938.
12 L J, P X, C, R G, N D, G S O2 . ACS N 2013;7(7):6001-6.
13 J SH, A S, G A. L 2017;56:15520-38.
14 I T, S K, K M, T T, T K, T . PCCP 2018;20(9):6024-33.
15 S K, D N, M C, V N, E J. T 2002;149(8):370-7.
16 C XH, S M, S WH, L G, H X, Q, S 2011;7(22):3163-8.
17 K H, G M, J L, H J, W C, C M. U . M 2019;1(4):1077-87.
18 S Q, F, X, L W, L H, L C 2017;29(31):1701583-90.
19 X X, G C, X L, T H, D, W T 2019. // /10.1021/ 9 08191.
20 C C, H B X, N J, C S, L F, 3D T 6A 4V : ff ;
21 S šć J, B žć D. T ff NB 316L SLM. S C T 2016;307:407-17.

22 R DC, HB, L J, L SJ, J W, R, M . M S E A-S 2020;771:138586-95.
23 L X, C W, A J, K S, N J, D, L S 2009;324(5932):1312-4.
24 C P, R WC, G LB, L BL, P SF, C HM. T fl 2011;10:424-8.
25 J SD, D S, G L, K JP, H JV, V K. I fl . JM P T 2019;270:47-58.
26 X W, H L, L T, D, C Q, F . Eff 2019;170:107697-708.
27 G DD, M W, W K, P R. L . I M R 2013;57(3):133-64.
28 L E, T S, C L, F A. Eff 316L (SLM) . JM P T 2017;249:255-63.
29 X S, W L, J, W P, C T 6A 4V. A P A: M S P 2018;124:685-98.
30 L M, S, D W, S C. I A S 316L . M D 2015;87:797-806.
31 L CLA, M S, T M, A RC, W PJ, L PD. T ff A M 2019;166:294-305.
32 T X, K T WQ, T J, D M, M D, R . α/β T-6A-4V. S R 2016;6:26039-48.
33 K H, T XP, L NH, T SB, C CK. G T-6A-4V . V P P 2016;11(3):183-91.
34 R fi HK, K NV, G H, S TL, S BE, M 6 4 2013;22(12):3872-83.
35 T X, K T J, V G, P QX, G . A T-6A-4V. J A C 2015;646:303-9.
36 R DA, M LE, M H . N 2011;59(10):4088-99.
37 X, W H. Eff C -2.4N -0.7S . J A C 2018;743:258-61.
38 K S. W S E 2003;23:309-48.
39 L G, G J ff R, G N P. E C (111). N L 2010;10(9):3512-6.
40 L XS, C WW, C L, R ff R S. E N C 2009;9(12):4268-72.
41 XW, X C, X, W H, SQ, L. A . C 2020;161:479-85.
42 F AC, M JC, S V, C C, L M, M F, R . P R L 2006;97(18):187401-4.
43 S, G, J SH, F PC, H HQ. fi 2017;200:97-100.
44 J K, H, J, C J, D . F C -N CNT . A S S 2014;311:351-6.
45 R JV K, M DP, A C, M S, S MK. E EMI . C P A 2018;12:475-84.
46 S B, L W, W. C (EMI) . ACS A M I 2016;8(12):8050-7.
47 H N, 307.5S , 307.5S (L) - X, G OTT 11 S L J5.3(D)-310 1 537TD T ((

53 M 2019;34(5):489-98.
W B, C M, L M. R . A M

54 C H, W S, J , J, X, C J, S ff F₃O₄
2014;26:3484-9.
2019;121:139-48.
W L, J, Q. T ff MWCNT
-MWCNT . J M S : M B

56 D X , P GR, H P, Q F, M B , ML. Effi . J. M
2015;26(3):1895-9.

57 C 2012;22:18772-4.
HB, Q, WG, H X, T . ACS A M I

58 S A, U N, T V. T
2011;3:918-24.
M R 2016. // /10.1051/ /2016021.

59 P MT, J H, R ff RS, S L. T . N L
2012;12:2959-64.

60 J K, H, H , D . P C -N M L
2017;122:244-7.

61 R H, L S, B S, K TW, L DS, L HJ, T
. S R 2015. // /10.1038/ 12710.
62 XT, F SG, L , G Q, L G, R KP, S
3D /
. M S E A-S 2020. // /10.1016/J
.2019.105670.

63 R DA, M LE, M E, H DH, M JL, M BI, .
N
M 2011;59(10):4088-99.
64 E SF, L KC, S VK, M IC. T . J T
E 1973;1(1):10-38.